The Physics of Organic Microcavity Light Emitting Diodes

A. Dodabalapur and L.J. Rothberg

Bell Laboratories, Lucent Technologies, 700 Mountain Avenue, Murray Hill, NJ 07974, USA

There has been a lot of progress made in the study of the modification of spontaneous emission by planar microcavities in a number of semiconductors, both inorganic [1] and organic [2-6]. The principal effect of the microcavity on the spontaneous emission is to redistribute the photon density of states such that only certain wavelengths, which correspond to allowed cavity modes, are emitted in a given direction. The spontaneous emission intensity is enhanced in the direction normal to the cavity axis relative to a non-cavity device. The external quantum efficiency or integrated intensity may also be enhanced in some cases. The conditions under which efficiency enhancement occurs are described later in the article. There is also an angular dependence to the emission wavelength, linewidth, and intensity.

The use of electroluminescent organic materials as the active medium in planar microcavities results in a number of interesting and potentially useful optical effects. The electroluminescent molecule 8-hydroxyquinoline aluminum (Alq) has been the subject of many recent reports on organic LEDs. Undoped Alq has a fairly broad free space emission spectrum covering the range 450-650 nm, and LEDs with external quantum efficiencies of 0.3-1.3 % photons/electron have been made with Alq together with a hole transporting material such as triphenyl diamine (TAD). The Alq/TAD system, in which only the Alq emits light in a LED device, is used in most of the experiments described in this article.

The schematic structure of a typical microcavity LED is shown in Figure 1. The bottom mirror usually consists of a dielectric quarter wave stack. The stop band of the QWS must be wide enough to cover the free space spectral range of the electroluminescent semiconductor used. The width of the stop band is approximately $\lambda.\Delta n/n$ where Δn is the index difference between the layers that constitute the stack, λ is the center wavelength of the stop band and n is the average index. Using a pair of dielectrics with a high index difference results in a broad stop band. The peak reflectivity of the stack (R_2) is given by [4]:

$$R_2 = \tanh \sum_i \tanh^{-1}(r_i) \qquad (1)$$

where r_i is the index difference between a pair of layers in the stack. The total optical thickness of the cavity, L, is given by:

$$L(\lambda) \approx \frac{\lambda}{2}\left(\frac{n}{\Delta n}\right) + \sum_j n_j L_j + \left|\frac{\varphi_m}{4\pi}\lambda\right| \qquad (2)$$

The first term in Eq. 2 is the penetration depth of the electromagnetic field into the dielectric stack, the second term is the sum of optical thicknesses of the layers between the two mirrors and the last term is the effective penetration depth into the top metal mirror.

Of paramount importance, for a number of applications, is the relative intensity of light emitted from a microcavity LED in comparison with light emitted from a non-cavity LED possessing the same active layer structure. In a typical non-cavity organic/polymeric LED the emissive and transport layers are placed above ITO-coated glass. An analysis of the optics in such a LED structure has shown that only a fraction $1/2n^2$ (n ~ substrate index of refraction) of the total light generated escapes through the back of the glass into air [7].

The rest of the light is internally reflected and either escapes through a waveguide mode or is reabsorbed. The use of the microcavity LED architecture offers a way to alter this emission pattern; indeed, in some cases an enhancement in intensity can be achieved.

The relative comparisons between intensities of cavity and non-cavity devices was made using two techniques. The experimental data was supplemented by detailed theoretical calculations. In the first set of experiments, the external quantum efficiency of both the cavity and non-cavity LEDs are measured by placing a large area Si photodiode very close to the back of the glass substrate. A large fraction of the total light emitted through the back of the substrate into air is absorbed by the photodiode, which has a known responsivity. In this manner comparisons can be made of the integrated intensities. Such measurements were made for several sets of devices including cavity LEDs with different on-axis resonance wavelengths and non-cavity LEDs.

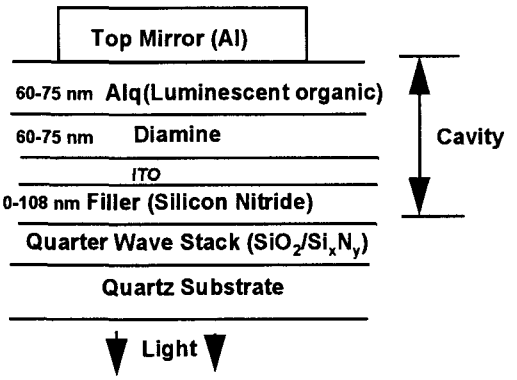

Figure 1 Schematic structure of a cavity LED.

In Fig.2 (a)-(c) are shown the electroluminescence spectra measured along the cavity axis for three cavity LEDs possessing different resonance wavelength. These spectra are typical of many others measured on the same patterned substrate. The LEDs possess identical active layer dimensions; it is only the patterned Si_3N_4 filler that creates differences in the optical thickness of the cavity. The emissive material is undoped Alq. Also shown in each of the figures is the external quantum efficiency as measured with the Si photodiode. The external quantum efficiency, which is a measure of the integrated intensity of light that exits though the back of the substrate, is extracted from the L-I characteristics. For comparison, non-cavity LEDs have an external quantum efficiency of 0.32-0.4 %, which is only slightly more than those of the cavity LEDs. The cathode metal/top mirror is Al in both the cavity LEDs and the reference non-cavity LEDs. It can be noticed in Fig. 2 (b), that two modes contribute to the light collected by the photodiode. However, over most angles of interest, devices (a) and (c) are substantially single mode. The small peak near 460 nm in (a) is very weak and disappears over most angles away from the cavity axis. Thus, our results indicate that that the integrated intensities in cavity and non-cavity in which Alq is the emissive material are essentially similar. Before we discuss the significance of this result, we describe below the details of the second set of experiments to compare intensities in cavity and non-cavity devices.

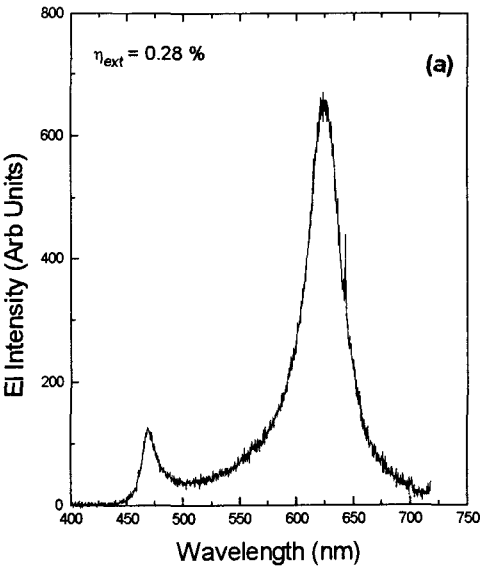

Figure 2a Electroluminescence spectrum from a cavity LED with two modes: a weak mode at 460 nm and a strong mode at 625 nm.

In these experiments two different substrates were employed: one quartz substrate with a 3-period SiO_2/Si_3N_4 quarter wave stack and the other plain quartz. 30 nm of ITO was deposited on both substrates by pulsed laser deposition of a commercial ITO target in 1 mTorr of O_2 at a substrate temperature of 250 ^{0} C. This was followed by depositing 60 nm of TAD and ~ 60 nm of Alq, and then defining arrays of 1 mm diameter Al dots on each of the two substrates. Thus, the two sets of devices - cavity and non-cavity - possess identical layer structures (including the ITO) which were deposited simultaneously. The LEDs were then excited by a constant current source, and the light emitted collected by a high transmission liquid light guide placed some distance away from the back of the glass substrate along the cavity axis. The light guide is positioned so as to only collect light very close to the cavity axis (collection angle < 10 degrees). The collected light is dispersed in a 0.5 m spectrometer and detected with a liquid nitrogen cooled CCD detector. Several cavity and non-cavity LEDs were excited by equal injection currents and their on-axis EL spectra recorded for the same period of time (10 s). The on-axis resonance wavelength for the cavity LEDs is 570 nm. The angular intensities (intensities over a small angular range) of the cavity and non-cavity LEDs are almost identical.

The enhancement of the emission intensity along the cavity axis (at the resonance wavelength) is given by [1]:

$$G_e = \frac{\varsigma}{2}\frac{\left(1+\sqrt{R_1}\right)^2\left(1-R_2\right)}{\left(1-\sqrt{R_1R_2}\right)^2}\frac{\tau_{CAV}}{\tau} \qquad (3)$$

where R_2 is the reflectivity of the top (metal) mirror, R_1 is the reflectivity of the dielectric mirror, and ς is the antinode enhancement factor. ς has a maximum value of 2 when the emitting dipoles (i.e. exciton recombination zone) is located exactly at the antinode of the standing wave. τ_{cav}/τ is the ratio of exciton lifetimes in the cavity device and the non-cavity device. Thus we can make a first order approximation that $\tau_{cav} \sim \tau$. The value of R_1R_2 can be found from the equation:

$$Q = \frac{\lambda}{\Delta\lambda} = \frac{2\pi L}{\lambda}\left[-\ln\left(R_1R_2\right)^{0.5}\right]^{-1} \qquad (4)$$

which relates the Q of the cavity to the resonance wavelength (λ), cavity optical thickness (L), and mode linewidth ($\Delta\lambda$). From Equation 4 , $(R_1R_2)^{1/2} = 0.69$, which is lower than what was originally expected. Taking $R_1 = 0.8$, $R_2 = 0.6$, and $\varsigma = 1.4$ (since the exciton recombination zone is spread over about 20 nm), gives $G_e = 4.9$, which agrees quite well with the measured value of 4.1. The agreement is even closer if τ_{cav}/τ is taken to be 0.9. If the cavity resonance wavelength was in the range 520-550 nm instead of 570 nm, the angular enhancement would have been 1.3 along the cavity axis. This small increase would be a result of better alignment between the maximum intensity band of the Alq free space emission spectrum and the microcavity resonance.

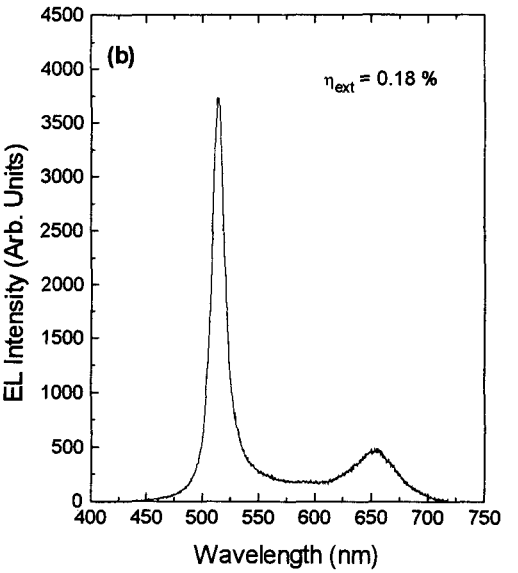

Figure 2b Electroluminescence spectrum with modes at 515 nm (strong) and 655 nm (weak).

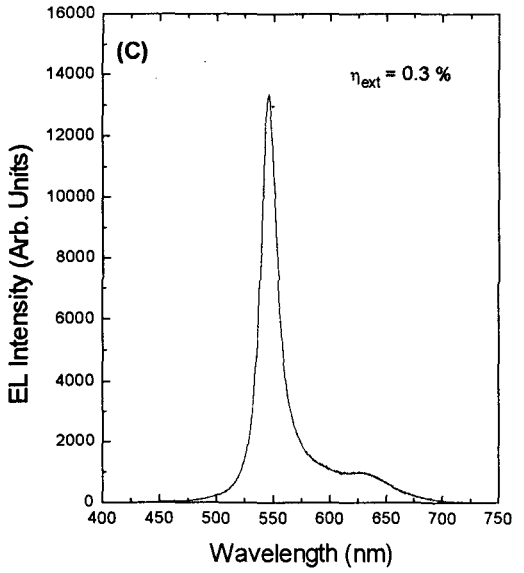

Figure 2c Single mode electroluminescence spectrum.

The Important changes to the emission spectrum of an electroluminescent organic material produced by planar microcavity effects have been described. In cavity devices with an Alq emissive layer it is possible to realize saturated colors with peak wavelengths in the range 495-625 nm and a variety of unsaturated colors including white. The patterned planar microcavity scheme to realize full-color organic LED based displays has been described. The external quantum efficiency (or integrated intensity) of cavity devices were carefully measured and for single mode LEDs are slightly lower than those of equivalent non-cavity device.

REFERENCES

1. E.F. Schubert, N.E.J. Hunt, M. Micovic, R.J. Malik, D.L. Sivco, A.Y. Cho, and G.J. Zydzik, Science **265**, 943 (1994).

2. N. Takada, T. Tsutsui, and S. Saito, Appl.Phys. Lett. **63**, 2032 (1993).

3. T. Nakayama, Y. Itoh, and A. Kakuta, Appl. Phys. Lett. **63**, 594 (1993).

4. A. Dodabalapur, L.J. Rothberg, T.M. Miller, and E.W. Kwock, Appl. Phys. Lett. **64**, 2486 (1994).

5. A. Dodabalapur, L.J. Rothberg, and T.M. Miller, Electron. Lett. **30**, 1000 (1994).

6. A. Dodabalapur, L.J. Rothberg, and T.M. Miller, Appl. Phys. Lett. **65**, 2308 (1994).

7. N.C. Greenham, R.H. Friend, and D.D.C. Bradley, Adv. Mater. **6**, 491(1994).